Research Article Vol. 9, No. 9 / September 2021 / Photonics Research 1715

PHOTONICS Research

Widely tunable, high-power, femtosecond noncollinear optical parametric oscillator in the visible spectral range

Robin Mevert,[1,2,*] Yuliya Binhammer,[1,2] Christian M. Dietrich,[1,2] Luise Beichert,[1,2] José R. Cardoso de Andrade,[1,2] Thomas Binhammer,[3] Jintao Fan,[1,2] and Uwe Morgner[1,2]

[1]Institute of Quantum Optics, Leibniz University Hannover, Welfengarten 1, D-30167 Hannover, Germany
[2]Cluster of Excellence PhoenixD, Welfengarten 1, D-30167 Hannover, Germany
[3]neoLASE GmbH, Hollerithallee 17, D-30419 Hannover, Germany
*Corresponding author: mevert@iqo.uni-hannover.de

Received 26 March 2021; revised 23 May 2021; accepted 9 June 2021; posted 11 June 2021 (Doc. ID 426107); published 19 August 2021

Ultrafast visible radiation is of great importance for many applications ranging from spectroscopy to metrology. Because some regions in the visible range are not covered by laser gain media, optical parametric oscillators offer an added value. Besides a high-power broadband laser source, the ability to rapidly tune the frequency of pulses with high-power spectral density offers an extra benefit for experiments such as multicolor spectroscopy or imaging. Here, we demonstrate a broadband, high-power, rapidly tunable femtosecond noncollinear optical parametric oscillator with a signal tuning range of 440–720 nm in the visible range. The oscillator is pumped by the third harmonic of an Yb-fiber laser at 345 nm with a repetition rate of 50.2 MHz. Moreover, the signal wavelength is tuned by changing the cavity length only, and output powers up to 452 mW and pulse durations down to 268 fs are achieved. This is, to the best of our knowledge, the first demonstration of a quickly tunable femtosecond optical parametric oscillator that covers nearly the entire visible spectral range with high output power.

https://doi.org/10.1364/PRJ.426107

1. INTRODUCTION

Frequency tunable femtosecond sources such as optical parametric oscillators (OPOs) are of great interest in various applications, e.g., coherent anti-Stokes Raman spectroscopy (CARS) [1], multiphoton microscopy [2], frequency comb metrology [3], and terahertz generation [4]. They are available in various wavelength ranges: the ultraviolet (UV) [5], visible (VIS) [6], near-infrared (NIR) [7], and midinfrared (MIR) region [8]. VIS OPOs are of particular importance, because the visible spectral range cannot be covered by a tunable source with typical laser gain media. Until now, it has been quite difficult and elaborate to realize a fast frequency-tunable laser source with high output powers and a broad wavelength range in the visible range. One approach is to generate fiber-optic Cherenkov radiation in a tapered photonic crystal fiber. A resulting tuning range of 414–612 nm with output power below 5.5 mW was reported in Ref. [9].

Over the past decades, crystal materials like beta barium borate (BBO), periodically-poled lithium niobate and bismuth triborate were used in synchronously pumped OPOs. Some of these reports addressed the intracavity second harmonic of the signal or sum-frequency generation of the signal and pump inside near-infrared OPOs [10–14]. As a result of the high fundamental power in these cases, up to a few hundred milliwatts of average output power have been achieved. However, the tuning range was limited to the phase-matching bandwidth of the second harmonic and sum-frequency-generation process, so that high output powers have been achieved only over a small wavelength range.

Others have reported pumping an OPO with blue light from the second harmonic of a Ti:Sa laser to create tunable femtosecond laser pulses directly in the visible range [6,15,16]. However, due to the limited pump power, the output power was small. Recently, this idea was taken up again utilizing harmonics of Yb-doped thin disk oscillators and fiber lasers [7,17] for higher pump powers.

Comparing the different wavelength tuning schemes in OPOs, methods like varying the internal crystal angle [6] or the crystal temperature [12] require seconds before stable operation at the new wavelength is reached. A much quicker way to tune the wavelength is by changing the cavity length and therefore the group delay between the pump and a chirped signal pulse–in particular when combined with an ultrabroadband noncollinear phase-matching scheme. Based on this method, the authors' group has demonstrated tuning speeds beyond

100 nm/ms [18] in a near-infrared noncollinear parametric oscillator (NOPO).

Noncollinear phase matching in BBO can be realized by a constant angle $\pm\alpha$ between the pump and signal beams in two different configurations. At first, the Poynting vector walk-off compensation (PVWC) geometry is characterized by a small angle between the Poynting vectors of the pump and signal with a better spatial overlap. A major disadvantage is a crossing of the second-harmonic phase matching curve of the signal, which is responsible for a strong dip in the tuning power (here at 615 nm). Second, at $-\alpha$, in the tangential phase-matching geometry (TPG), the Poynting vectors of the idler and pump point in similar directions, which causes a stronger walk-off of the signal. More information about these cases can be found in the literature [19,20].

In this work, we demonstrate a high-power, high-repetition-rate quickly tunable noncollinear optical parametric oscillator, which covers almost the entire visible spectral range (VIS-NOPO). It is directly pumped by the third harmonic of an Yb-fiber laser at 345 nm with up to 3 W of pump power. Due to the noncollinear phase-matching scheme, the signal wavelength can be changed from deep blue up to the red, from 440 to 720 nm by varying the cavity length only. Long-time stable output powers up to 452 mW with 1.4% rms power fluctuations are obtained. Without extra pulse compression effort, the shortest signal pulse duration is 286 fs.

2. EXPERIMENTAL SETUP

Figure 1 shows a schematic sketch of the experimental setup. It consists of an Yb-fiber pump laser with an average output power of up to 22 W at 1040 nm, a repetition rate of 50.2 MHz, and pulse durations of 250 fs. Next, the third harmonic of the Yb-fiber laser at 345 nm is created in two steps. The second harmonic of the pump laser is generated in a BBO crystal ($\theta = 23.2°$, $L = 1.5$ mm) in one arm and combined with the fundamental from a second arm via sum-frequency mixing in a second BBO crystal ($\theta = 32.5°$, $L = 1$ mm). The generated third harmonic at 345 nm can be scaled up to 3 W of average output power with an overall efficiency of 17%.

The pump beam is then focused into a Brewster-cut BBO crystal ($\theta = 39°$, $L = 2$ mm) inside the VIS-NOPO cavity. A noncollinear angle of $\alpha = 4.5°$ in the PVWC geometry is set for ultrabroadband phase matching. The cavity consists of six plane and two curved (ROC = −150 mm; $d = 25.4$ mm) doubly chirped mirrors (DCMs) with high reflectivity and defined dispersion in the range of 400–700 nm. The mirrors together with the gain crystal flatten the group-delay dispersion (GDD) curve close to zero, and a BK7-substrate ($L = 3$ mm) placed in Brewster's angle in the cavity introduces a well-defined net GDD. An output coupler with 14% transmission in the spectral window from 480 to 720 nm is placed at the end of the cavity. The other end mirror is mounted on a piezo-driven translation stage, which is used to tune the cavity length.

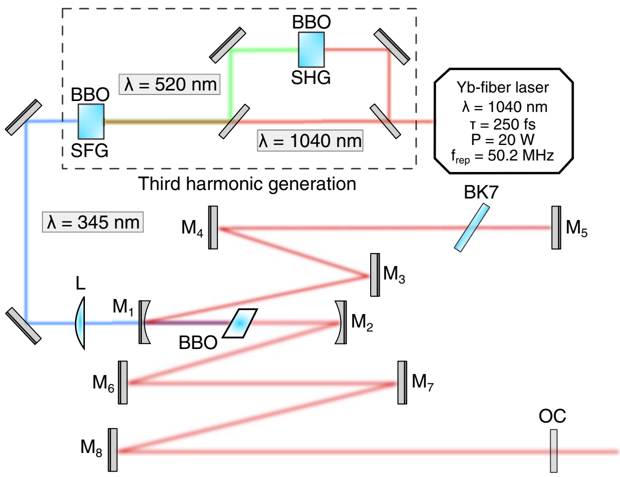

Fig. 1. Schematic setup of the VIS-NOPO. The upper part of the sketch shows the pump laser and the third-harmonic-generation setup. A pump lens L ($f = 200$ mm) focuses the third harmonic into the Brewster-cut BBO crystal ($\theta = 39°$; $L = 2$ mm), which is surrounded by two curved DCMs (M_1 and M_2: $d = 25.4$ mm; ROC = −150 mm) with a spectral transmission window at 345 nm. Moreover, a BK7 substrate (uncoated, $L = 3$ mm) is inserted into the cavity, which consists of six additional plane DCMs (M_3–M_8) and an output coupling mirror (OC) with 14% transmission from 480 to 720 nm.

3. RESULTS

Figure 2 shows the recorded signal spectra, output powers, and pulse durations of the VIS-NOPO as a function of the cavity length. Changing the cavity length by 400 μm results in a signal tuning range from 440 to 720 nm. The green line in Fig. 2(a) represents the calculated GD of all intracavity elements. NOPO tuning traces this curve quite nicely; even beyond 700 nm, it follows the drift in the DCM dispersion curve.

In Fig. 2(b), pulse durations from a second-harmonic intensity autocorrelator (sech^2-shape assumed) and output powers

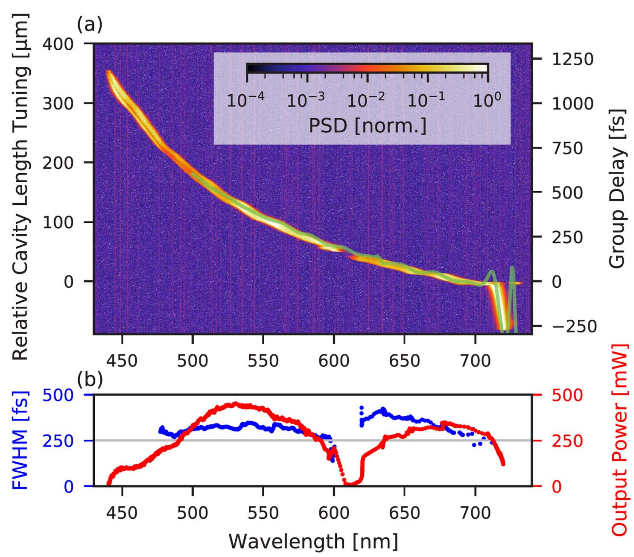

Fig. 2. Tuning behavior of the VIS-NOPO. (a) Measured power spectral density (PSD) as a function of wavelength and cavity length/group delay. The green line indicates the calculated net intracavity GDD. (b) Measured pulse durations and output powers.

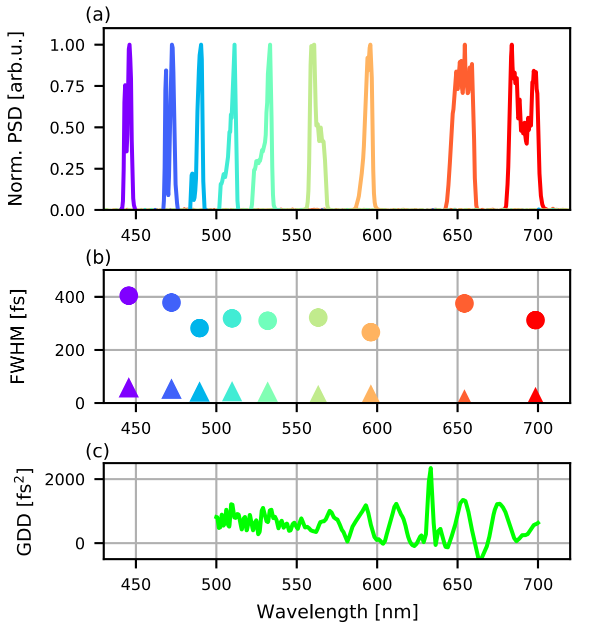

Fig. 3. (a) Normalized signal spectra for different cavity lengths. (b) Measured pulse durations (circles) and calculated Fourier limits (triangles). (c) Green line: calculated GDD.

are shown. The output power rises up to a maximum of 452 mW at 530 nm; between 604 and 620 nm, the signal power decreases drastically due to the generation of the parasitic second harmonic from the PVWC geometry. Except that dip, the output power stays above 170 mW over a range from 475 to 700 nm. Due to the sensitivity of the autocorrelator, the pulse duration could only be determined reliably at higher output powers. It is roughly constant at 490–600 nm and 620–700 nm around 300 to 400 fs without extra pulse compression efforts.

Figure 3(a) shows selected representative signal spectra; Fig. 3(b) shows the corresponding Fourier limits and the measured pulse duration. The quiet constant pulse width over the whole tuning range is a result of the net dispersion curve shown in Fig. 3(c). Here, the green solid line reflects the calculated GDD of all cavity elements. Due to the cavity dispersion, the signal pulses are positively chirped. However, external pulse compression by additional extra-cavity DCM bounces would result in pulse durations below 120 fs over the whole tuning range.

Figure 4 illustrates the scaling of the signal output power by variation of the incident pump power. The resulting curve shows no sign of saturation at a slope efficiency of 23.7% and a pump threshold of $P_{\mathrm{th}} = 960$ mW. In these numbers, the reflection losses of the pump on the crystal surface of 19.4% are not subtracted. This measurement promises further power scalability of the NOPO concept. During the experiments, no direct damage of the crystal material was observed. However, the two-photon absorption of the BBO sets an upper limit to the pump intensity inside the crystal. Moreover, the coating on the curved DCM could be damaged by high intensities. The beam profile of the signal at the maximum output power is recorded and inserted

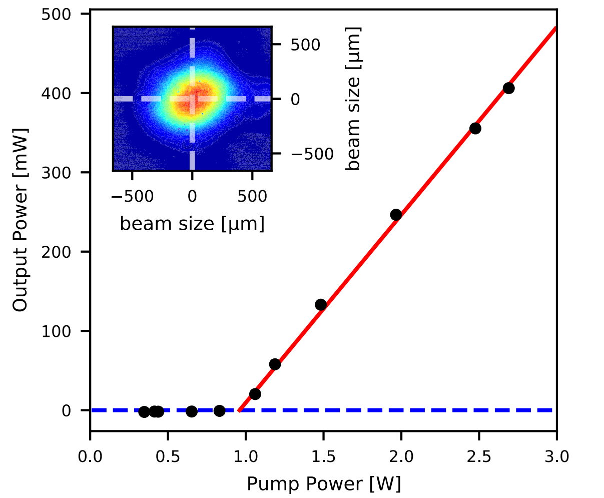

Fig. 4. Measured slope efficiency and threshold of the signal at 530 nm. The solid red line illustrated a linear fit. Inset: signal beam profile at maximum output power.

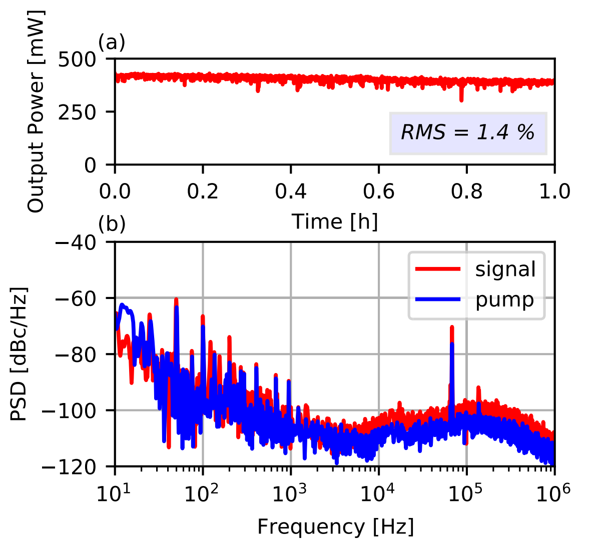

Fig. 5. (a) Long-term stability measurement of the signal output power. (b) Phase noise PSD of signal and pump.

into Fig. 4. It shows a slightly elliptical beam shape, which is attributed to a similar ellipticity in the pump beam.

In Fig. 5(a), the power evolution at 530 nm at the highest pump and signal power is plotted over a period of 1 h, whereas in Fig. 5(b), the phase noise power spectral density (PSD) of the signal and pump is shown over a range from 10 Hz to 10 MHz. The latter is obtained by a spectrum analyzer (Agilent E4440a). The slight degradation in output power is caused by a simultaneous degradation in pump power during the measurement. The determined rms noise of 1.4% is smaller than the pump rms noise of 4.1%. Further, the PSD is smaller at low frequencies; at high frequencies, the NOPO cavity inherits the phase noise almost entirely from the pump. Higher stabilities might be achievable with better passive stability and an active control of the pump and stabilization of the NOPO cavity length.

4. CONCLUSION AND OUTLOOK

In conclusion, we have demonstrated a high-power, quickly tunable noncollinear optical parametric oscillator that covers nearly the complete visible spectral range. It is directly pumped by the third harmonic of an Yb-fiber laser. The signal wavelength can be tuned from 440 to 720 nm by changing the cavity length only. Output powers of up to 450 mW with less than 1.4% rms fluctuations over a period of 1 h and pulse durations down to 270 fs are obtained. The parasitic generation of the second harmonic of the signal causes the output power to drop to a minimum of 8 mW between 604 and 620 nm. This effect could be eliminated by utilizing the TPG, but this would result in a bad beam profile of the signal. Scalability of the NOPO concept is possible by proper cavity design to counteract the two-photon absorption of the UV light in the BBO crystal and the damage threshold of the curved mirror coatings. This makes the VIS-NOPO a great option for ultrafast spectroscopy and the generation of high-power frequency combs. For these applications, the beam pointing stability, beam quality, and tuning speeds would need to be investigated in more detail. Moreover, high tuning speeds of over 100 nm/ms could enable new methods for two-color spectroscopy and imaging.

Funding. Deutsche Forschungsgemeinschaft (MO 850/31-1, MO 850-19/2, MO 850-23/1); Germany's Cluster of Excellence PhoenixD (EXC 2122, Project ID 390833453); European Union's Horizon 2020 research and innovation program under the Marie Sklodowska-Curie Agreement (713694).

Disclosures. The authors declare no conflicts of interest related to this paper.

REFERENCES

1. C. Cleff, J. Epping, P. Gross, and C. Fallnich, "Femtosecond OPO based on LBO pumped by a frequency-doubled Yb-fiber laser-amplifier system for CARS spectroscopy," Appl. Phys. B **103**, 795–800 (2011).
2. V. Andresen, S. Alexander, W.-M. Heupel, M. Hirschberg, R. M. Hoffman, and P. Friedl, "Infrared multiphoton microscopy: subcellular-resolved deep tissue imaging," Curr. Opin. Biotechnol. **20**, 54–62 (2009).
3. Y. Kobayashi, K. Torizuka, A. Marandi, R. L. Byer, R. A. McCracken, Z. Zhang, and D. T. Reid, "Femtosecond optical parametric oscillator frequency combs," J. Opt. **17**, 094010 (2015).
4. J. E. Schaar, K. L. Vodopyanov, and M. M. Fejer, "Intracavity terahertz-wave generation in a synchronously pumped optical parametric oscillator using quasi-phase-matched GaAs," Opt. Lett. **32**, 1284–1286 (2007).
5. C. Gu, M. Hu, J. Fan, Y. Song, B. Liu, L. Chai, C. Wang, and D. T. Reid, "High power tunable femtosecond ultraviolet laser source based on an Yb-fiber-laser pumped optical parametric oscillator," Opt. Express **23**, 6181–6186 (2015).
6. M. Ghotbi, A. Esteban-Martin, and M. Ebrahim-Zadeh, "BiB_3O_6 femtosecond optical parametric oscillator," Opt. Lett. **31**, 3128–3130 (2006).
7. T. Lang, T. Binhammer, S. Rausch, G. Palmer, M. Emons, M. Schultze, A. Harth, and U. Morgner, "High power ultra-widely tuneable femtosecond pulses from a non-collinear optical parametric oscillator (NOPO)," Opt. Express **20**, 912–917 (2012).
8. C. F. O'Donnell, S. C. Kumar, P. G. Schunemann, and M. Ebrahim-Zadeh, "Femtosecond optical parametric oscillator continuously tunable across 3.6-8 μm based on orientation-patterned gallium phosphide," Opt. Lett. **44**, 4570–4573 (2019).
9. X. Liu, J. Laegsgaard, R. Iegorov, A. S. Svane, F. O. Ilday, H. Tu, S. A. Boppart, and D. Turchinovich, "Nonlinearity-tailored fiber laser technology for low-noise, ultra-wideband tunable femtosecond light generation," Photon. Res. **5**, 750–761 (2017).
10. Y. Khanukaeva, T. Lang, A. Tajalli, J. R. Andrade, T. Binhammer, and U. Morgner, "Efficient fast-tunable femtosecond visible radiation based on intracavity sum-frequency generation in a NIR NOPO," in *Conference on Lasers and Electro-Optics (CLEO)* (IEEE, 2016), paper STh1P.6.
11. X. P. Zhang, J. Hebling, J. Kuhl, W. W. Rühle, and H. Giessen, "Efficient intracavity generation of visible pulses in a femtosecond near-infrared optical parametric oscillator," Opt. Lett. **26**, 2005–2007 (2001).
12. T.-Y. Jeong, S.-H. Kim, G.-H. Kim, and K.-J. Yee, "Visible-pulse generation in gain crystal of near-infrared femtosecond optical parametric oscillator," Opt. Express **23**, 25620–25627 (2015).
13. D. T. Reid, M. Ebrahimzadeh, and W. Sibbett, "Efficient femtosecond pulse generation in the visible in a frequency-doubled optical parametric oscillator based on $RbTiOAsO_4$," J. Opt. Soc. Am. B **12**, 1157–1163 (1995).
14. R. J. Ellingson and C. L. Tang, "High-power, high-repetition-rate femtosecond pulses tunable in the visible," Opt. Lett. **18**, 438–440 (1993).
15. G. M. Gale, M. Cavallari, and F. Hache, "Femtosecond visible optical parametric oscillator," J. Opt. Soc. Am. B **15**, 702–714 (1998).
16. T. J. Driscoll, G. M. Gale, and F. Hache, "Ti:sapphire second-harmonic-pumped visible range femtosecond optical parametric oscillator," Opt. Commun. **110**, 638–644 (1994).
17. J. Fan, C. Gu, C. Wang, and M. Hu, "Extended femtosecond laser wavelength range to 330 nm in a high power LBO based optical parametric oscillator," Opt. Express **24**, 13250–13257 (2016).
18. T. Lang, T. Binhammer, S. Rausch, G. Palmer, M. Emons, M. Schultze, A. Harth, and U. Morgner, "Rapidly spectral ramping of an ultra-wide tuneable femtosecond non-collinear optical parametric oscillator (NOPO) with high average output power," in *Laser Applications to Chemical, Security and Environmental Analysis* (OSA, 2012), paper AT2A.2.
19. G. Cerullo and S. de Silvestri, "Ultrafast optical parametric amplifiers," Rev. Sci. Instrum. **74**, 1–18 (2003).
20. T. Lang, A. Harth, J. Matyschok, T. Binhammer, M. Schultze, and U. Morgner, "Impact of temporal, spatial and cascaded effects on the pulse formation in ultra-broadband parametric amplifiers," Opt. Express **21**, 949–959 (2013).